

Transmission Electron Microscopic Study of Whisker Formation on Tetracalcium Phosphate in Hydrochloric Acid

Kuan-Liang Lin^{*1}, Jiin-Huey Chern Lin and Chien-Ping Ju^{2,*2}

Department of Materials Science and Engineering, National Cheng-Kung University, Tainan 70101, Taiwan, R.O. China

The present study investigates the changes in microstructure and microchemistry (particularly Ca/P ratio) during whisker formation on the surface of TTCP powder in hydrochloric solution. XRD results indicate that the as-fabricated (non-treated) powder has a monolithic TTCP crystal structure. When the powder is treated for 10 min in HCl, a DCPD phase appears on TTCP surface, which increases in intensity with treating time. When treated longer than 4 h, the DCPD intensity decreases. When treated for 24 h, the DCPD phase disappears. TEM results indicate that, when TTCP is treated for 10 min, fine globular-shaped DCPD crystals are observed to precipitate on the surface of TTCP particles. When treated for 1 h, hexagonal Ca-deficient apatite whiskers with an average Ca/P ratio of 1.5 form. With treating time the apatite whiskers continue to grow in size and increase in Ca/P ratio. When treated for 24 h, the length and thickness of the apatite whiskers can reach >500 and >50 nm, respectively, with an average Ca/P ratio of 1.8. The microchemical data indicate that the apatite whiskers grown on the surface of TTCP particles are substantially non-stoichiometric in nature. Compressive strength data indicate that apatite whiskers grown on TTCP surface under a favorable condition can largely improve the properties of the resulting CPC.

(Received June 18, 2004; Accepted August 17, 2004)

Keywords: tetracalcium phosphate (TTCP), calcium phosphate cement (CPC), transmission electron microscopy (TEM), whisker

1. Introduction

Due to its superior biocompatibility and osteoconductivity, calcium phosphate cement (CPC) has been suggested to be used as a filling material in dental and orthopedic applications.¹⁻⁷⁾ One major advantage of CPC is its capability to be easily shaped in paste form during operation or injected into a cavity with a syringe without requiring an open way through tissues. The primary reaction product of most CPCs after being implanted for a while is various kinds of apatite,⁸⁾ which is the main inorganic component of human bones and teeth.^{9,10)}

Tetracalcium phosphate (TTCP), a member of the calcium phosphate family, is a popular candidate precursor of apatite¹¹⁾ and frequently used as a component of CPC powder.^{12,13)} TTCP is known to have a high chemical activity and reacts at room temperature with acidic aqueous solution.¹⁴⁾ The obtained set/hardened material has a high affinity for the living body and is useful for many applications.¹⁵⁾

The combination of TTCP and DCPA (or DCPD) powders is one of the most popular formula of CPC used today.¹⁶⁻¹⁸⁾ It is generally accepted that the setting mechanism of TTCP/DCPA-based CPC involves formation of apatite crystals.^{8,19-23)} Ishikawa and Asaoka²¹⁾ suggested that dissolved calcium and phosphate ions from both powders in water are precipitated in the form of hydroxyapatite (HA) on the powder surface. Brown and Fulmer¹⁹⁾ suggested that, in TTCP/DCPA-based CPC, only the earliest nuclei can have a stoichiometric HA composition. Further growth of the nuclei causes the apatite phase to become calcium-deficient with a Ca/P ratio near 1.5.

In a transmission electron microscopic (TEM) study on the setting mechanism of TTCP/DCPA-based CPC in an acidic phosphate solution, Chen *et al.*²⁴⁾ suggested that the early-stage apatite formation involves quick dissolution of a

surface layer of TTCP particles due to its relatively high dissolution rate in the solution. The dissolved calcium and phosphate ions, along with those ions readily in the solution, are then precipitated predominantly on the surface of DCPA powder. During the later stages of reaction, the extensive growth of apatite whiskers effectively links DCPA particles together and also bridges the larger TTCP particles, causing the CPC to be set and not dissolve when immersed in Hanks' solution. The same authors further revealed that a whisker-treated TTCP/DCPA-based CPC has a higher apatite formation rate, denser structure, and higher compressive strength than that without the whisker treatment.²⁵⁾

Although the whisker treatment in the study of Chen *et al.*^{24,25)} has been shown very effective in enhancing the properties of TTCP/DCPA-based CPC, the simultaneous reactions between both powders and phosphate solution as well as the existence of phosphate ions readily in the solution cause analysis of the results to be complicated. To eliminate such complications and single out the effect of whisker treatment on TTCP in acidic solution, the present study investigates the changes in microstructure and microchemistry (particularly Ca/P ratio) during whisker formation on the surface of a monolithic TTCP powder in an acidic, Ca and P-free hydrochloric solution using TEM technique.

2. Materials and Methods

The TTCP powder used for the study was fabricated in-house from the reaction of dicalcium pyrophosphate ($\text{Ca}_2\text{P}_2\text{O}_7$) (Sigma Chem. Co., St. Louis, MO, USA) and calcium carbonate (CaCO_3) (Katayama Chem. Co., Tokyo, Japan) by a weight ratio of 1:1.^{27,26)} The powders were mixed uniformly in ethanol, followed by heating in an oven to let the powders dry. The dried powder mixture was then heated to 1400°C to allow two powders to react to form TTCP.

In order to study the whisker formation behavior at different stages of treatment, 1 gm TTCP powder was mixed

^{*1}Graduate Student, National Cheng-Kung University

^{*2}Corresponding author, E-mail: ju_servantofchrist@yahoo.com

in 13 ml, 0.16 kmol/m^3 HCl solution with a pH value of 0.8 for a series of times (10 min, 1 h, 4 h, 12 h and 24 h) at room temperature. After treatment the powder was vacuum-filtered and washed with de-ionized water twice, followed by drying in an oven. For TEM examination, the dried powder was supersonically dispersed in ethanol. A drop of the powder-dispersed ethanol was dripped on a 3 mm-diameter, #325 mesh carbon grid and let dry. The specimen was then coated with a thin carbon film for electrical conductivity for TEM examination.

A JEOL JEM-3010 scanning transmission electron microscope (STEM) operated at 200 kV was used for the study. An energy dispersive spectroscopy (EDS) system (Link II Energy Dispersive X-ray Analysis System, England) attached to the microscope was used to determine the chemistry (particularly Ca/P ratio) of the whiskers at different stages of treatment. Microdiffraction (typically with a spot size of 15–25 nm for the study) was performed to help identify the crystal structure of individual whiskers.

X-ray diffraction (XRD) was also carried out to help identify the phase changes during various stages of whisker treatment. A Rigaku D-MAX B X-ray diffractometer (Tokyo, Japan) with Ni-filtered $\text{CuK}\alpha$ radiation operated at 30 kV and 20 mA at a scanning speed of $0.25^\circ/\text{min}$ was used for the study. The various phases were identified by matching each characteristic XRD peak with that compiled in JCPDS files.

To evaluate the effect of whisker treatment on the compressive strength of monolithic TTCP-derived CPC, the whisker-treated TTCP powder was mixed with 3 M diammonium hydrogenphosphate ($(\text{NH}_4)_2\text{HPO}_4$) hardening solution with a pH value of 8.6 and liquid/powder ratio of 0.35 ml/gm. After mixing for 1 min, the cement paste was uniformly packed in a stainless steel mold under a popularly-used pressure of 0.7 MPa. This mold has an opening of 6 mm in diameter and 12 mm in depth (ASTM F 451-99a) for the preparation of samples for compressive strength testing. After mixing for 15 min, the CPC samples were removed from the mold and immersed in 20 ml Hanks' physiological solution²⁷⁾ at 37°C for 24 hours.

3. Results and Discussion

Figure 1 shows typical XRD patterns of TTCP powder with and without whisker treatment. As can be seen from the figure, the original TTCP (without whisker treatment) has a TTCP crystal structure. When the monolithic TTCP powder was whisker-treated for 10 min in 0.16 kmol/m^3 HCl solution, a DCPD phase appeared. Although TTCP and DCPD have many crystallographic planes with similar "d values", the presence of DCPD (020) unmistakably indicates the presence of DCPD phase. This monoclinic DCPD phase increased in intensity with treating time until 4 h, after that the DCPD intensity decreased. When the TTCP was treated for 24 h, the DCPD phase disappeared. This variation in DCPD intensity is quantitatively demonstrated in DCPD (12-1)/TTCP (121) peak height ratios in Fig. 2.

As also indicated in the XRD patterns, when the powder was whisker-treated for 1 h, an apatite phase started to be observed, as identified by the right "shoulder" of TTCP (130) peak. This hexagonal apatite phase continued to grow

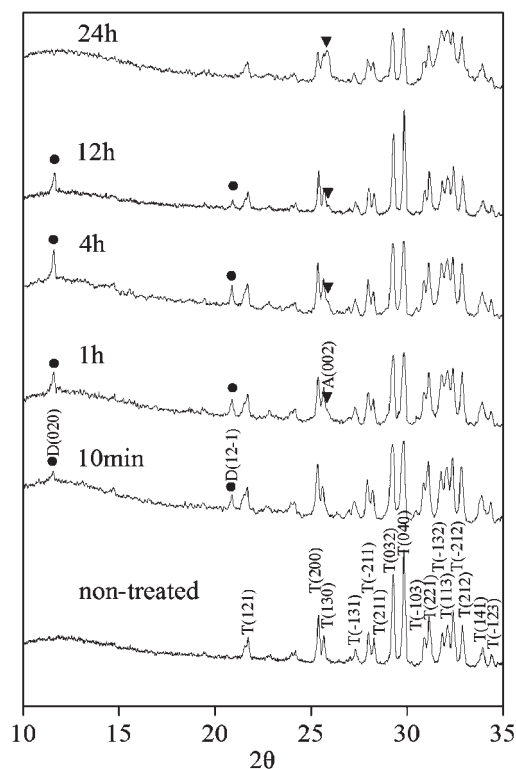


Fig. 1 XRD patterns of non-treated and whisker-treated TTCP. (T: TTCP; A: apatite; D: DCPD).

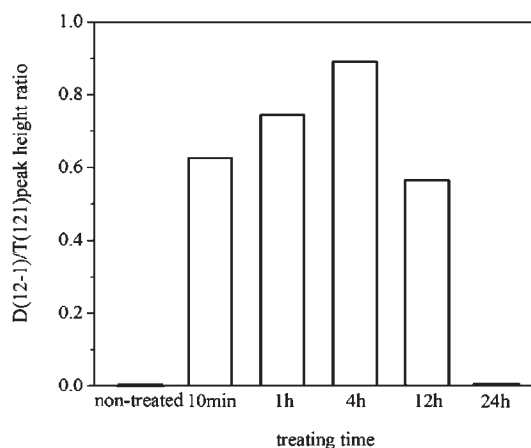


Fig. 2 D(12-1)/T(121) XRD peak height ratios of whisker-treated TTCP.

with whisker-treating time, as can be clearly seen from the increasing apatite (002) peak intensity.

It was reported that TTCP dissolves in acid solution easier than DCPD and can cause an initial increase in pH value of the solution.²⁸⁾ This statement is supported by the measurement of Chen *et al.*²⁴⁾ indicating that the early stage dissolution rate of TTCP is about 5 times higher than DCPA in an acidic phosphate-based solution. This large difference in dissolution rate between TTCP and DCPA in acidic solution may explain the quick formation of DCPD phase. The observed increase in apatite intensity at the expense of DCPD with increasing whisker-treating time is probably due to the growing reaction between TTCP and DCPD to form apatite that continues to consume the earlier-precipitated

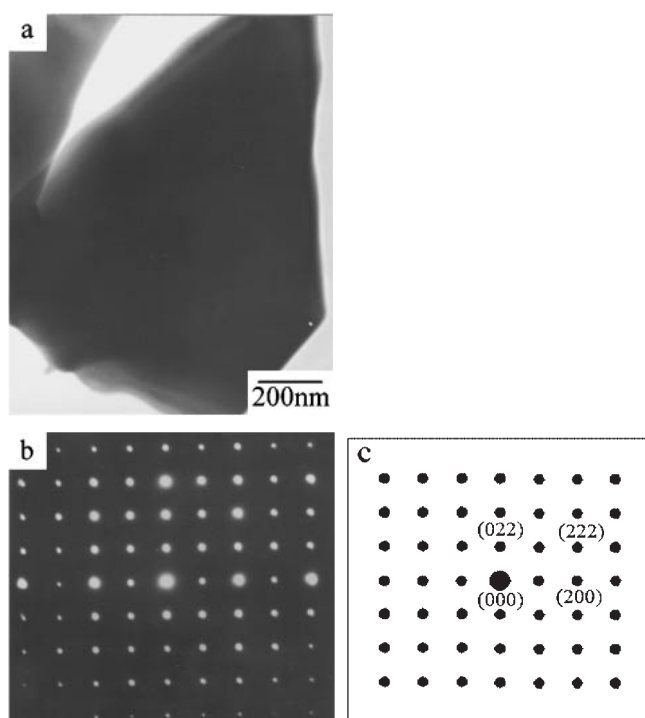


Fig. 3 BF image (a), [01-1] zone SAD pattern (b) and index (c) of non-treated TTCP.

DCPD phase.

Figure 3 shows the typical morphology and electron diffraction pattern of an as-fabricated, monolithic TTCP particle. As shown in the bright field (BF) micrograph (Fig. 3a), the surface of the non-whisker-treated particle was neat and clean. The selected-area diffraction (SAD) pattern (Fig. 3b) and its index (Fig. 3c) clearly show that the particle has a crystal structure of TTCP.

After whisker-treatment for 10 min, fine DCPD crystals were observed to precipitate on the surface of TTCP particles, as shown in Fig. 4. The BF image (Fig. 4a) and dark field (DF) image of the same area (Fig. 4b) indicate that the early stage DCPD crystals are globular-shaped. Exact sizes of these fine crystals are hard to determine due to extensive overlapping of the crystals. A rough estimate from the images indicates that the diameters of the majority of such globular crystals are less than 50 nm. The Moiré fringes seen in the DF image are a result of the overlapping of the crystals. The fringes being substantially parallel across almost every crystal (Fig. 4b) is believed to result from a large number of such fine crystals with very similar orientation precipitated on the surface of a single TTCP grain. If this statement is true, it seems that the precipitated DCPD crystals have a strong orientation relationship with the parent TTCP crystal- at least during early stage precipitation.

The measurement of lattice images further confirms that the observed fine crystals are indeed DCPD crystals. For example, as shown in Fig. 4c, the measured lattice spacing values, 0.76, 0.50, 0.26 and 0.25 nm, are very close to the theoretical values of DCPD (020) (0.759 nm), (110) (0.492 nm), (150) (0.262 nm) and (23-1) (0.2519 nm), respectively. The average atomic Ca/P ratio of such fine DCPD crystals obtained from the EDS-microchemical analysis

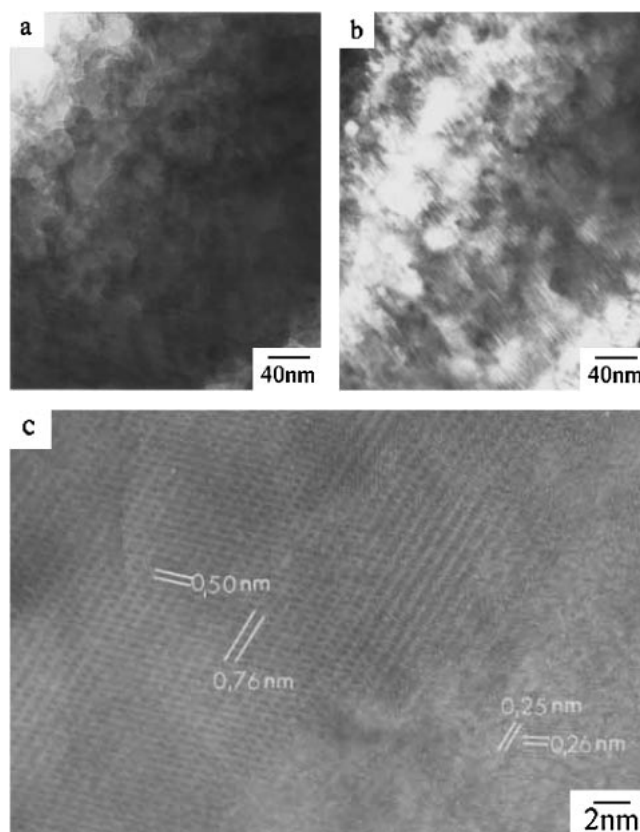


Fig. 4 BF image (a), DF image (b) and lattice image (c) of 10 min-treated DCPD particles on TTCP surface.

using scanning mode with a spot size of 15 nm was found to be about 1.5, which is considerably higher than the theoretical Ca/P ratio of DCPD (1.0). It is worth noting, however, that this Ca/P ratio might be overestimated due to the possibility for the nano-sized DCPD crystals to overlap the parent TTCP particle during analysis.

As mentioned earlier, when TTCP was whisker-treated for 1 h, apatite started to be observed. The formation of the apatite is considered as a result of the reaction between TTCP and DCPD phases. The formation of apatite is again confirmed by TEM examination. As shown in Fig. 5a, the formation of apatite whiskers on the surface of TTCP powder being treated for 1 h is evident. The length and thickness of majority of these whiskers are <200 nm and <20 nm, respectively. The “spotted ring” SAD pattern (Fig. 5b) obtained from an area of 0.4 μm is due to a large number of whiskers with different orientations contributing to form the diffraction pattern.

Although most “d values” of apatite phase are quite close to those of DCPD and TTCP, the presence of apatite (110) ring (more clearly shown in the original film), as indexed in Fig. 5c, clearly indicates the presence of apatite phase. Microdiffraction patterns (with a spot size of 25 nm) of individual whiskers further confirm that the whiskers are apatite with a hexagonal crystal structure. An example of the microdiffraction pattern of an apatite whisker and its index is demonstrated in Figs. 5d and 5e. During the microanalysis of the outgrown apatite whiskers, the diffraction of early stage globular-shaped DCPD crystals was overshadowed by the

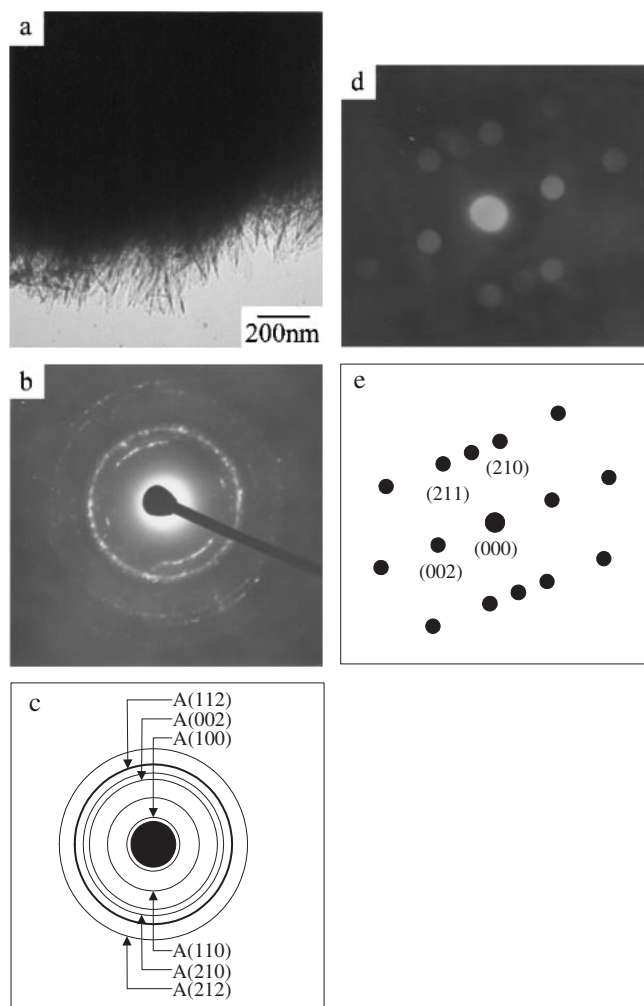


Fig. 5 BF image (a), SAD pattern (b) and index (c), $[-120]$ zone microdiffraction pattern (d) and index (e) of 1 h-treated apatite whiskers on TTCP surface.

large number of the whiskers.

The average Ca/P ratio of 1 h-treated apatite whiskers was found to be 1.50, indicating that the apatite at this stage was Ca-deficient apatite. The earlier-mentioned potential overlapping effect on the determination of Ca/P ratio during the microchemical analysis of DCPD crystals was largely eliminated for the microanalysis of apatite whiskers due to their larger sizes and the greater distances of the analyzed spots to TTCP surface.

With treating time the apatite whiskers continued to grow. According to Chen *et al.*,²⁴⁾ during the setting process of CPC, the extensive growth of apatite whiskers could effectively bridge the calcium phosphate particles and cause the cement to be set. An example for the morphology and diffraction of 12-h whiskers is demonstrated in Fig. 6. Both microdiffraction patterns of individual whiskers and spotted-ring SAD patterns (more clearly shown in the original film) of numerous whiskers again confirm that these whiskers are of apatitic phase. The average Ca/P ratio under this treatment was about 1.6. When treated for 24 h, the length and thickness of the apatite whiskers could be greater than 500 and 50 nm, respectively. The Ca/P ratio of the whiskers was also observed to increase with treating time. When treated for

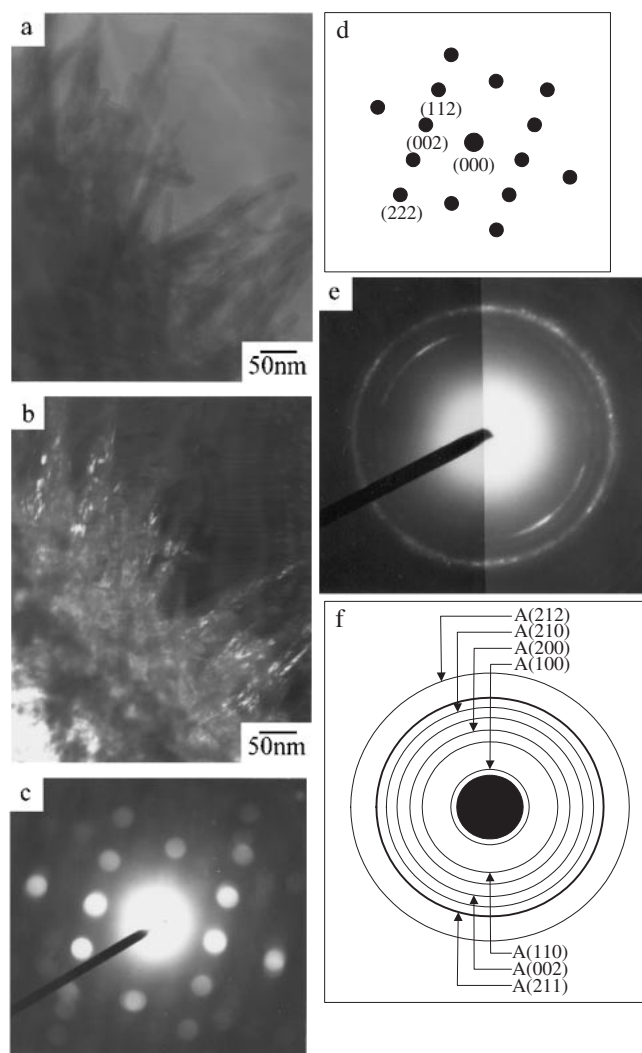


Fig. 6 BF image (a), DF image (b), microdiffraction pattern (c) and index (d), SAD pattern (e) and index (f) of 12 h-treated apatite whiskers on TTCP surface.

24 h, the average Ca/P ratio of the whiskers increased to 1.8. The present Ca/P ratio data indicate that the apatite whiskers grown on the surface of TTCP particles are chemically non-stoichiometric in nature.

As discussed in earlier studies,^{24,25)} the powder-liquid reaction time (and thus the whisker dimensions) is critical to the properties of the resulting CPC. It was suggested that, while calcium phosphate particles are locked in place by the bridging apatite whiskers, the cement is set and will not dissolve when immersed in Hanks' solution.

As demonstrated in Fig. 7, the compressive strength of CPC prepared from the present whisker-treated TTCP powder increases with treating time up to 12 h, where the maximum strength is found. When the TTCP powder was treated for 24 h, the compressive strength of the resulting CPC largely declined. Apparently the 12 h-treated apatite whiskers are most effective in enhancing the strength of the resulting CPC. Chow and Takagi²⁹⁾ reported that anhydrously-prepared TTCP with a surface free from moisture-induced HA contaminant performed better than ordinary TTCP. With a somewhat different philosophy, the present study demon-

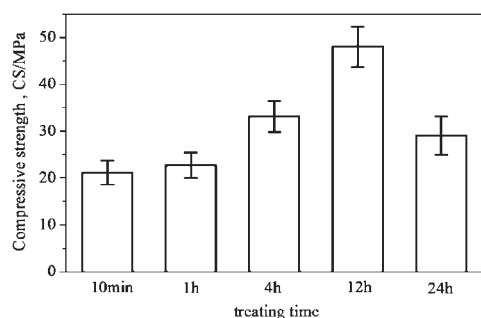


Fig. 7 One-day compressive strength of CPC derived from whisker-treated TTCP.

strates that apatite whiskers grown on TTCP surface under a favorable condition can largely improve the properties of the resulting CPC.

4. Conclusions

The XRD and TEM results indicate that, when TTCP powder was treated for 10 min in 0.16 kmol/m^3 HCl, fine globular-shaped DCPD crystals were observed to precipitate on the surface of TTCP particles. The intensity of DCPD increased with treating time. When treated for 1 h, hexagonal Ca-deficient apatite whiskers with an average Ca/P ratio of 1.5 formed. With treating time the substantially non-stoichiometric apatite whiskers continued to grow in size and increase in Ca/P ratio. When treated for 24 h, the length and thickness of the whiskers could respectively reach >500 and >50 nm with an average Ca/P ratio of 1.8, while the DCPD phase disappeared. The compressive strength data indicate that apatite whiskers grown on TTCP surface under a favorable condition could largely improve the properties of the resulting CPC.

REFERENCES

- 1) L. C. Chow: The Centennial Memorial Issue of The Ceramic Society of Japan **99** (1991) 954–964.
- 2) A. A. Chohayeb, L. C. Chow and P. J. Tsaknins: J. Endod. **13** (1987) 384–387.
- 3) P. D. Costantino, C. D. Friedman, K. Jones, L. C. Chow, H. J. Pelzer and G. A. Sisson: Arch. Otolaryngol. Head Neck Surg. **117** (1991) 379–384.
- 4) C. D. Friedman, P. D. Costantino, K. Jones, L. C. Chow, H. J. Pelzer and G. A. Sisson: Arch. Otolaryngol. Head Neck Surg. **117** (1991) 385–389.
- 5) Y. C. Hong, J. T. Wang, C. Y. Hong, W. E. Brown and L. C. Chow: J. Biomed. Mater. Res. **25** (1991) 485–498.
- 6) A. Sugawara, M. Nishiyama, K. Kusama, I. Moro, S. Nishimura, I. Kudo, L. C. Chow and S. Takagi: Dent. Mater. J. **11** (1992) 11–16.
- 7) C. Hamanish, K. Kitamoto, K. Ohura, S. Tanaka and Y. Doi: J. Biomed. Mater. Res. **32** (1996) 383–389.
- 8) Y. Miyamoto, K. Ishikawa, H. Fukao, M. Sawada, M. Nagayama, M. Kon and K. Asaoka: Biomaterials **16** (1995) 855–860.
- 9) M. J. Glimcher, L. C. Bonar, M. D. Grynpas, W. J. Landis and A. H. Roufosse: J. Cryst. Growth. **53** (1981) 100–119.
- 10) R. Z. LeGeros: Clin. Orthop. **395** (2002) 81–98.
- 11) S. R. Radin and P. Ducheyne: J. Biomed. Mater. Res. **27** (1993) 35–45.
- 12) K. Kurashina, H. Kurita, A. Kotani, H. Takeuchi and M. Hirano: Biomaterials **18** (1997) 147–151.
- 13) A. Yokoyama, S. Yamamoto, T. Kawasaki, T. Kohgo and M. Nakasu: Biomaterials **23** (2002) 1091–1101.
- 14) L. C. Chow and S. Takagi: Mat. Res. Soc. Symp. Proc. **179** (1991) 3–10.
- 15) A. Imura, T. Saito and S. Ikegami: U.S. Pat. No. 5,569,490.
- 16) M. T. Fulmer and P. W. Brown: J. Biomed. Mater. Res. **27** (1993) 1095–1102.
- 17) K. Ishikawa, S. Takagi, L. C. Chow and Y. Ishikawa: J. Mater. Sci. Mater. Med. **6** (1995) 528–533.
- 18) M. Otsuka, Y. Matsuda, Y. Suwa, J. L. Fox and W. I. Higuchi: J. Biomed. Mater. Res. **29** (1995) 25–32.
- 19) P. W. Brown and M. Fulmer: J. Am. Ceram. Soc. **74** (1991) 934–940.
- 20) K. S. TenHuisen and P. W. Brown: J. Dent. Res. **3** (1994) 598–606.
- 21) I. Ishikawa and K. Asaoka: J. Biomed. Mater. Res. **29** (1995) 1537–1543.
- 22) C. Liu, W. Shen, Y. Gu and L. Hu: J. Biomed. Mater. Res. **35** (1997) 75–80.
- 23) Y. Miyamoto, T. Toh, K. Ishikawa, T. Yuasa, M. Nagayama and K. Suzuki: J. Biomed. Mater. Res. **54** (2001) 311–319.
- 24) W. C. Chen, J. H. Chern Lin and C. P. Ju: J. Biomed. Mater. Res. **64A** (2003) 664–671.
- 25) W. C. Chen, C. P. Ju and J. H. Chern Lin: J. Oral. Rehabil. Accepted.
- 26) W. E. Brown and E. F. Epstein: J. Res. Nat. Bur. Stand. **69A** (1965) 547–551.
- 27) D. C. Mears: Internal. Metals Rev. **June** (1977) 119–154.
- 28) L. Xie and E. A. Monroe: Mat. Res. Soc. Symp. Proc. **179** (1991) 25–39.
- 29) L. C. Chow and S. Takagi: U.S. Pat. No. 5,542,973.